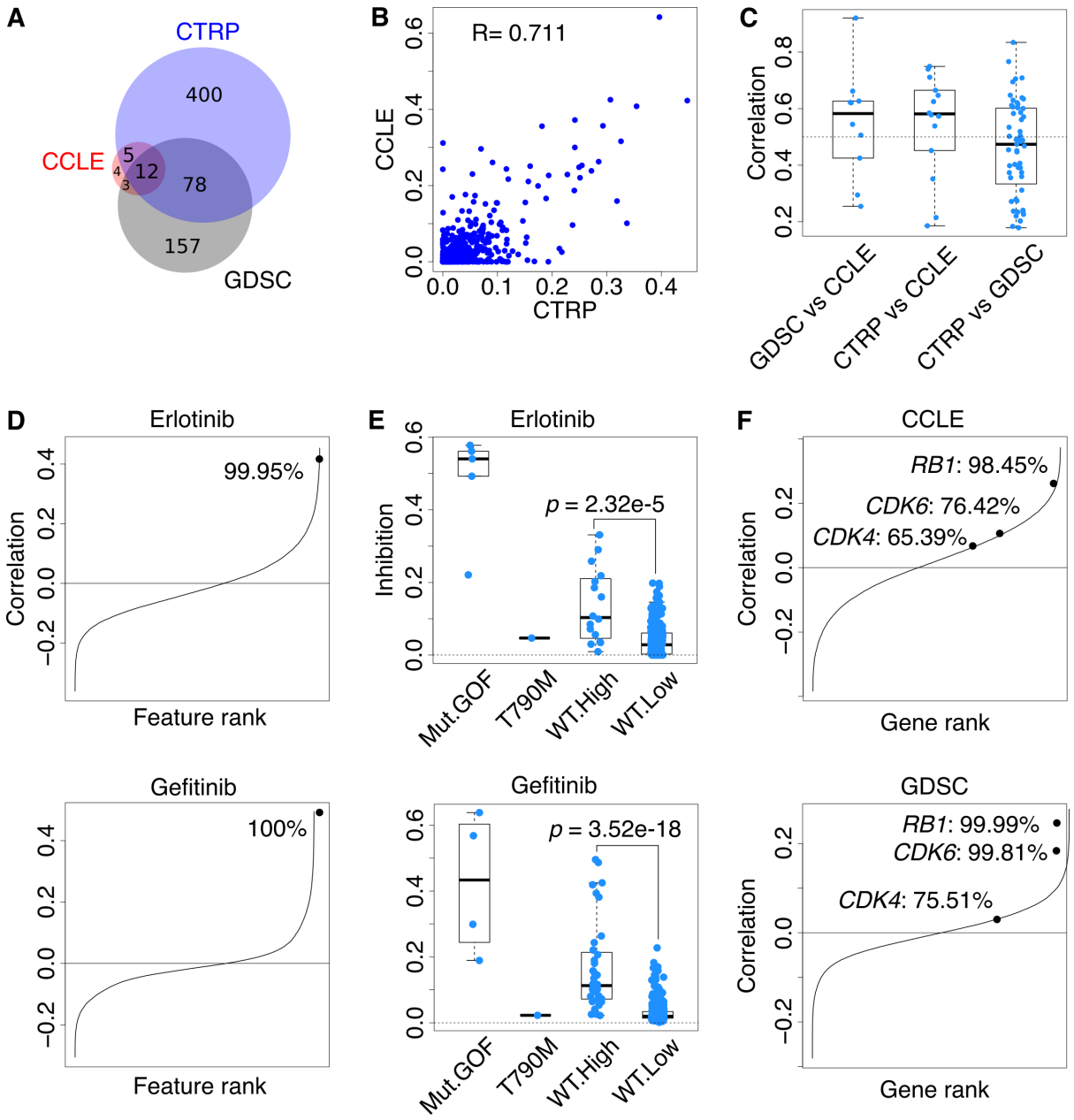

Figure S1. Compound screen data and drug target definition, Related to Figure 1.

(A) Overlap of compounds among three screen cohorts shown with Venn diagram. The numbers of compounds within sub-regions are also labeled.

(B) Consistency of PLX4720 response measurements between different cohorts. The drug response values, measured by area under dose response curve, are shown for PLX4720 across different cancer cell lines with CTRP results on X-axis and CCLE results on Y-axis. The consistency is computed with a Pearson correlation value.

(C) Consistency of drug response measurements among three cohorts. Between each combination of two cohorts, the Pearson correlations of drug response are shown for all targeted therapy compounds, with correlation 0.5 as the dotted reference line.

(D) Ordered correlations between gene features and *EGFR* inhibitor efficacy, with the relative position of *EGFR* expression marked as a black dot. Top: Erlotinib results in CCLE, Bottom: Gefitinib results in GDSC.

(E) *EGFR* inhibitor efficacy in different *EGFR* status groups. Top: Erlotinib results in CCLE, Bottom: Gefitinib results in GDSC. There are only five and four cell lines with

gain-of-function mutations (Mut.GOF, exon 19 in-frame and L858R) for CCLE and GDSC cohorts, respectively. There is one cell line with T790M mutation driving *EGFR* inhibitor resistance in both cohorts. For *EGFR* wild-type cell lines, the category "WT.High" consists of samples with *EGFR* expression two-fold greater than average, and "WT.Low" consists of samples with *EGFR* expression lower than average. The p-value is computed from the two-sided Wilcoxon rank-sum test.

(F) Ordered correlations between gene features and palbociclib efficacy, with the relative ranks of *RB1*, *CDK4* and *CDK6* labeled as black dots. Top: results in CCLE; Bottom: results in GDSC.

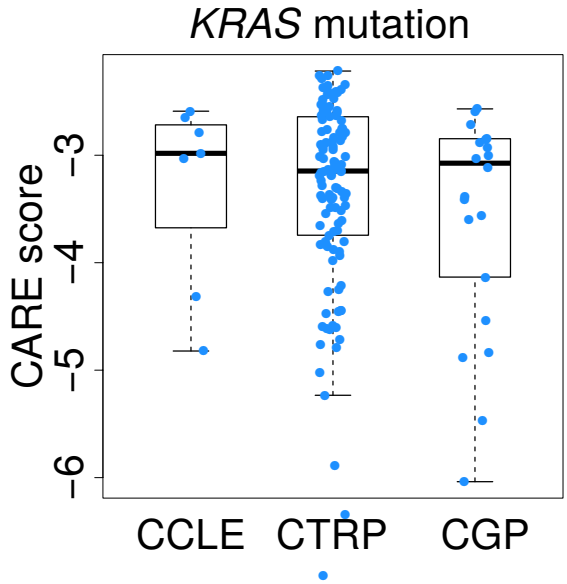

Figure S2. Significant CARE scores for *KRAS* mutation, Related to Figure 2.
Among all compounds screened in three cohorts, the statistically significant CARE scores are shown for *KRAS* mutation, with the median value as a thick bar in the box-plot. The bottom and top of the boxes are the 25th and 75th percentiles (interquartile range). Whiskers on the top and bottom represent the maximum and minimum data points within 1.5 times the inter-quartile range.

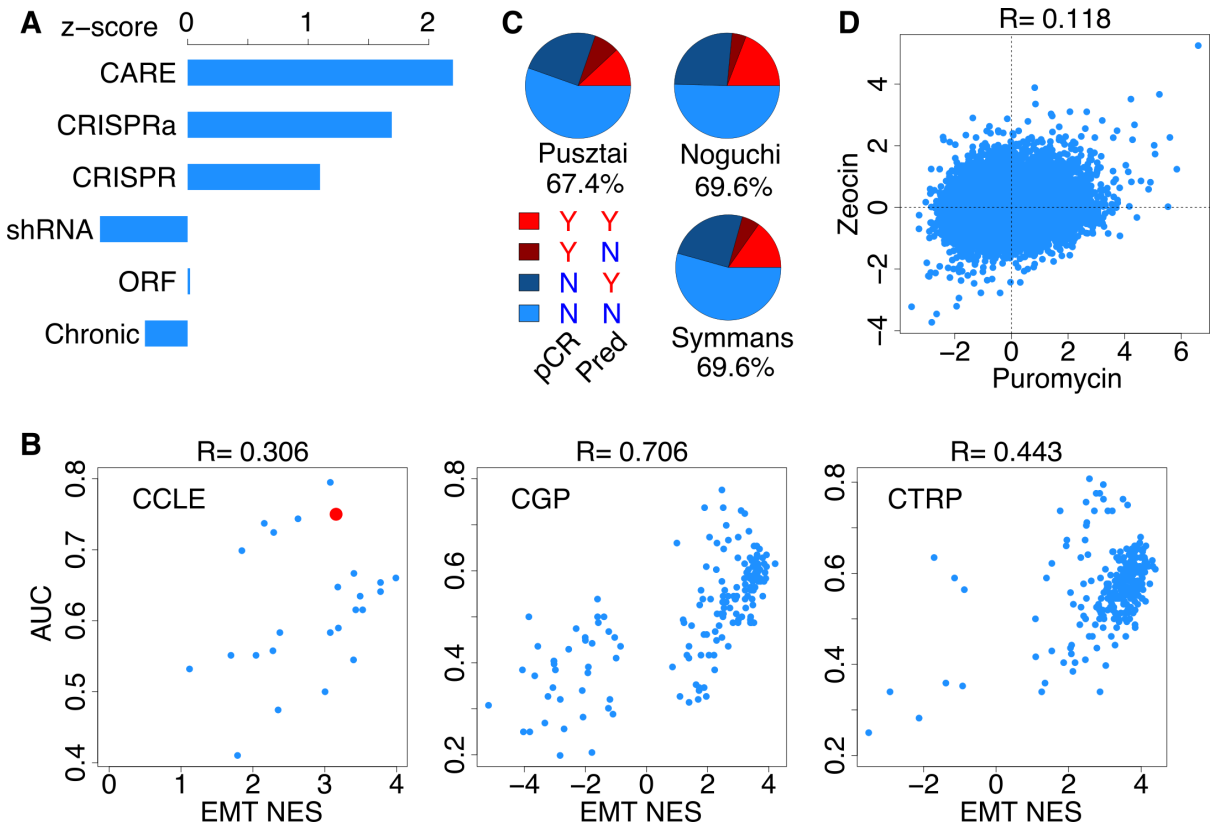

Figure S3. CARE can predict clinical outcome of targeted therapies, Related to Figure 3.

(A) Association between CARE signature and anti-BRAF clinical outcome. Using the clinical data of 12 patients treated with vemurafenib (Hugo et al., 2015), we applied the Cox-PH regression to test the association between each gene signature (Table S3A) and progress-free survival without any cutoff. The z-score of each signature (hazard coefficient/standard deviation) is used as a performance metric.

(B) Prediction performance on anti-*PD1* response correlates with the enrichment of EMT signature. For the CARE signature of each compound, its performance of predicting anti-*PD1* response was measured with area under ROC curve (AUC) (Figure 3). The enrichment of epithelial-to-mesenchymal (EMT) transition was the normalized enrichment score (NES) from the GSEA analysis software (Subramanian et al., 2005). In each screening cohort, the AUC and EMT enrichment of each compound are plotted on X and Y axes, with Pearson correlation between two axes as the title. The case of *BRAF* inhibitor on predicting anti-*PD1* response in Figure 3 was labeled with red dot in the CCLE plot.

(C) Prediction accuracy on paclitaxel response. All patients are classified into four sub-groups according to the status of pathological complete response (pCR) and predicted response (Pred), followed by the percentage of patients whose response status is consistent with CARE prediction.

(D) Consistency between replicates in CRISPRa screen. For the CRISPRa genome-wide screen (Konermann et al., 2015), the gene-wise fold change scores are shown for Puromycin selected replicate and Zeocin selected replicate. Pearson correlation between two replicates is shown as title.

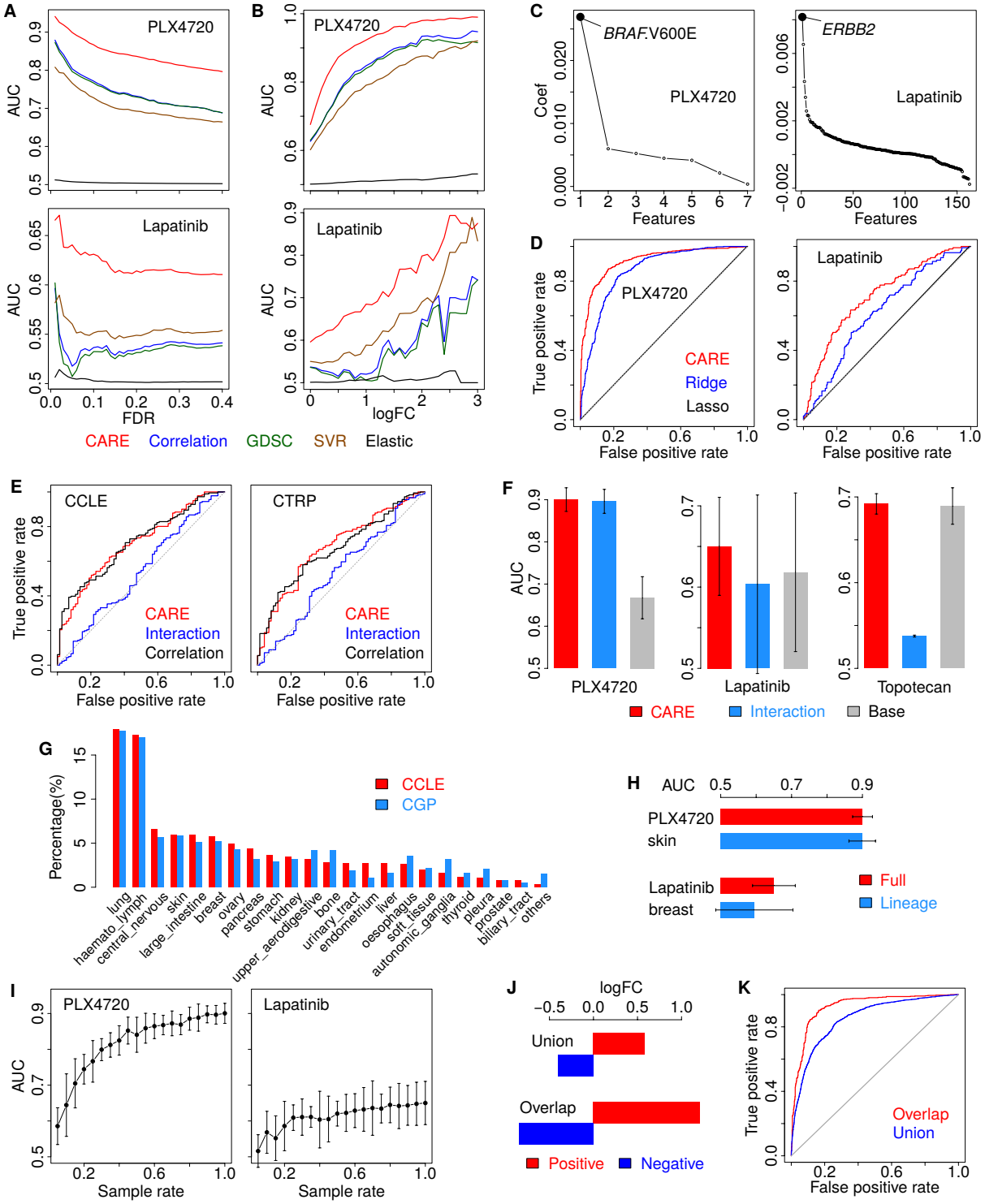

Figure S4. Performance comparison between CARE and other computational methods, Related to Figure 4.

(A) Performance comparison based on variations of evaluation standards. For each drug, the evaluation standard gene sets are selected with different thresholds of false discovery rate (FDR) computed by Limma (Ritchie et al., 2015). The area under ROC curve (AUC) of results from different computational methods are compared.

(B) Performance comparison as panel A with different thresholds of log-fold change (logFC) that tests the differential gene expression between drug-resistant and parental cell lines.

(C) Gene features selected by Elastic Net regression. The non-zero coefficients of Elastic Net are plotted for each drug in CCLE. Coefficients of drug target genes are highlighted with thick dots.
(D) Performance of Ridge and LASSO regression in predicting the gene expression signature of drug-resistant cell lines for PLX4720 and lapatinib.
(E) Performance of different models in predicting genes associated with topotecan resistance. The performance of CARE, Interaction and Correlation are compared using ROC curves.
(F) Performance AUC metrics for both interaction effects and base effects (Correlation normalized by its standard deviation) in CARE model on predicting genes associates with topotecan resistance. The mean values of three screen cohorts are shown, with standard deviations as error bars.
(G) Fractions of cell lines in different lineages of CCLE and GDSC (COSMIC) collections.
(H) CARE performance of lineage-specific analysis. PLX4720's chemical analog vemurafenib is primarily for skin cancer treatment, and lapatinib is mainly for breast cancer treatment. For each drug, the AUC metrics were shown for results using all cell lines and results using lineage-specific cell lines, with the mean and standard deviation (error bar) averaged among three screen cohorts.
(I) Performance of CARE after sub-sampling data. For each drug, the cell lines were sub-sampled, and the AUC metrics were computed under each sample rate. The mean and standard deviation were computed across three cohorts. A significant deterioration of performance happens after a down-sampling rate of 20%, which is higher than the fractions of most abundant lineage in panel G.
(J) Quality comparison between evaluation standard variations. Evaluation standard gene sets are created by taking either the union or overlap between two sets of differentially expressed genes in the drug-resistant M229-R5 and M238-R1 cell lines over their respective parental sensitive lines M229 and M238. To compare the quality of different evaluation standards, we used the differential gene expression profile of a third drug-resistant cell line SKMel28-R1 compared to its parental line SKMel28. The average log-fold changes (logFC) between SKMel28-R1 and its parental line are plotted for both positive and negative evaluation standards.
(K) Prediction performance of SKMel28-R1 expression on the "overlap" or "union" evaluation standard. In the ROC curves, the prediction performance on "overlap" set is consistently higher than the performance on "union" set.

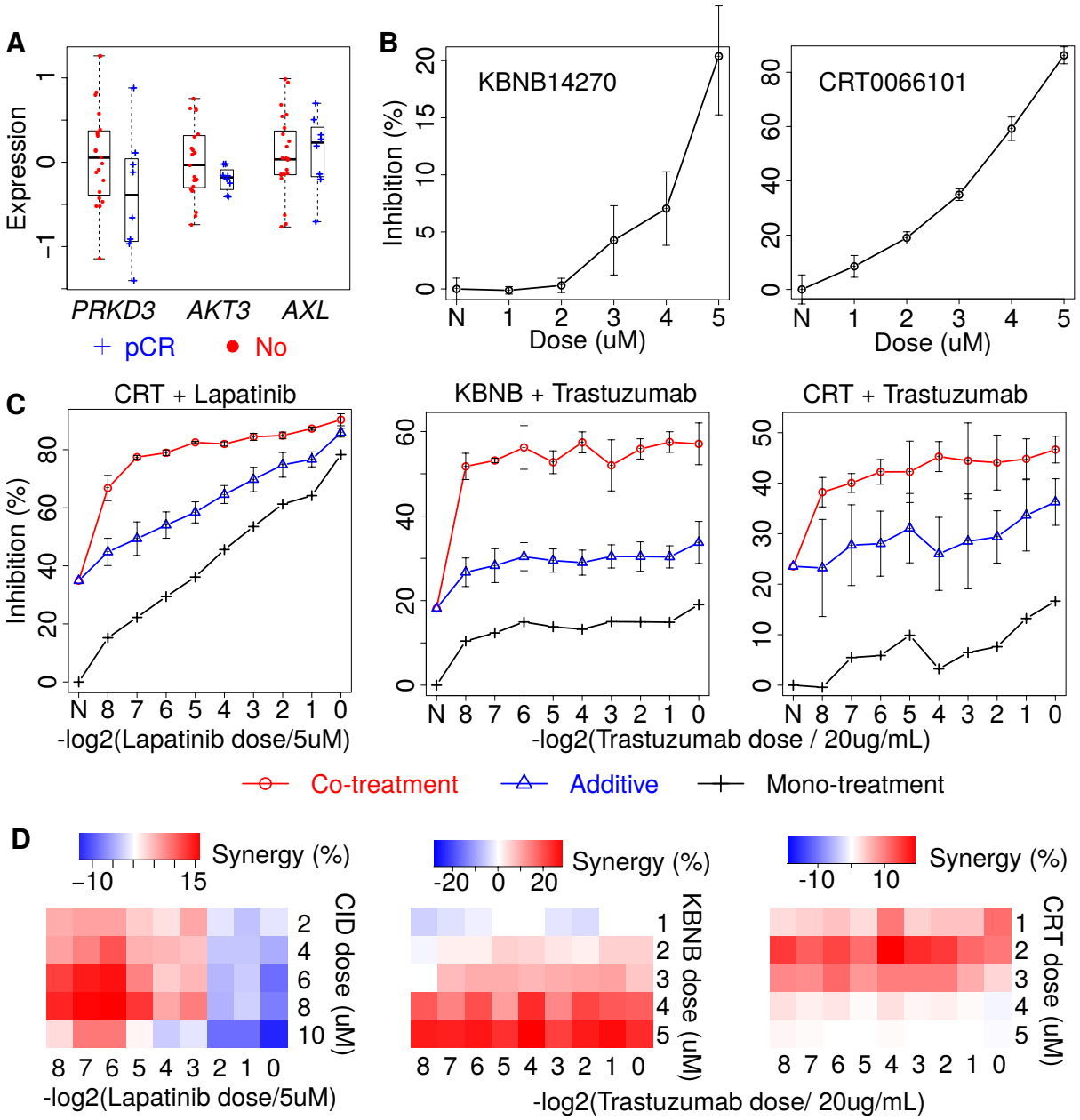

Figure S5. Inhibition of *PRKD3* increases anti-*HER2* efficacy, Related to Figure 5.

(A) Association between gene expression level and lapatinib clinical response. For each gene, the expression value is shown according to the pathological complete response status of patients, with median value in each group as a black bar. The bottom and top of the boxes are the 25th and 75th percentiles (interquartile range). Whiskers on the top and bottom represent the maximum and minimum data points within the range represented by 1.5 times the inter-quartile range.

(B) Inhibition effects on SKBR3 growth for *PRKD* inhibitors KBNB14270 and CRT0066101 at different concentrations. Each inhibition fraction was the median value from three replicate experiments with standard deviation as the error bar. N: none treatment control.

(C) Inhibition effects on SKBR3 growth for drug co-treatment compared with mono-treatment. The additive inhibition effect of co-treatment is estimated using Bliss independence model. Left: CRT0066101 in 3uM with lapatinib in different doses (2x dilution from 5uM); Middle: KBNB14270 in 5uM with trastuzumab in different

doses (2x dilution from 20ug/mL); Right: CRT0066101 in 2 uM with trastuzumab in different doses. N: none treatment control.

(D) Bliss synergy scores between combinations of anti-*HER2* drugs and *PRKD* inhibitors. Left: Lapatinib and CID2011756, Middle: Trastuzumab and KBNB14270, Right: Trastuzumab and CRT0066101.

Supplementary Tables

	Coef	Stderr	t-value	p-value
ERBB2	0.03951	0.00351	11.26	2.73E-26
EGFR	0.02004	0.00349	5.74	1.66E-08
AXL	-0.01828	0.00338	-5.41	9.67E-08
*AXL*ERBB2*	-0.0136	0.00333	-4.08	5.16E-05
*AXL*EGFR*	0.00386	0.00356	1.09	2.78E-01
CARE score *ERBB2*	-0.03188	0.00487	-6.55	1.44E-10
CARE score *EGFR*	-0.01442	0.00459	-3.14	1.78E-03

Table S1. Interaction test for multiple target genes of lapatinib, Related to Table 1 and Table 2.
The interactions between expression variables of lapatinib dual targets *ERBB2*, *EGFR* and the partner *AXL* are evaluated by linear regression with lapatinib efficacy as the outcome. The t-value is defined as regression coefficient divided by the standard error, and the p-value is calculated by the two-sided Student's t-test.

Cohort	Cell line	Compound
CCLE	495	24
CTRP	824	545
GDSC	990	250

Table S2. Number of cell lines and compounds in each cohort, Related to Figure 1.
The numbers of cell lines and compounds screened in each pharmacological cohort.

Treatment	Experiment	Genes	Pubmed	Data
PLX4720	CRISPRa screen	23722	25494202	Released
	CRISPR screen	17419	24336571	Released
	ORF screen	14457	24185007	Released
	shRNA screen	16126	23288408	Released
PLX4032	Chronic treatment	18547	21107323	Released
A. *BRAF*				

Lapatinib	Chronic treatment	20128	19671800, 24319068	Released
	shRNA screen	23742	19010894	No
	siRNA screen	337	23474757	Released
AEE788+shRNA	ORF screen	597	24909179	No
B. *ERBB2*				

anti-PD1+GVAX	In-vivo CRISPR screen in mice	830	28723893	Released
C. *PDCD1*				

Paclitaxel	Chronic treatment	18408	25199881	Released
	shRNA screen	74	17982636	No
	siRNA.1 screen	1187	25024437	Released
	siRNA.2 screen	21150	17429401	Released
	Clinical: Pusztai	12436	20064235	Released
	Clinical: Noguchi	20128	22320227	Released
	Clinical: Symmans	12436	21558518	Released
D. *TUBB*				

Table S3. Genomics signatures for clinical response prediction, Related to Figure 3.

For each targeted therapy, we collected published data related to drug response and resistance profiling. Column "Treatment" represents the drug used in an experiment. Column "Experiment" includes the brief description of experiments. CRISPR, shRNA, and siRNA are gene loss of function screens. ORF and CRISPRa are gene gain of function screens. For the in-vivo CRISPR screen on mice treated with immunotherapies, we translated all mouse top gene hits in supplementary table 1 of the publication (Manguso et al., 2017) into their human orthologs for further analysis. Chronic treatment represents differential gene expression profiling of drug resistant cell lines derived from chronic drug treatment compared with its parental sensitive cell lines. Column "Genes" tells the number of genes covered in each signature. Column "Data" indicates the availability of data with the study. If the data is not released, we extract the top gene hits reported in the publication as a gene set signature.

(A) *BRAF* inhibitors.

(B) *ERBB2* inhibitors.

(C) Anti-*PD1* antibody and GVAX vaccine.

(D) *TUBB* inhibitor paclitaxel.

		CCLE		CTRP		GDSC	
	Role	CARE	Elastic	CARE	Elastic	CARE	Elastic
EGFR	Resistant	-4.96	0	-4.62	0	-10.35	0
PDGFRB	Resistant	-4.67	0	0.24	0	-10.35	0
MET	Resistant	-2.91	0	-4.31	0	-3.16	0
YAP1	Resistant	-10.84	0	-7.54	0	-5.63	0
SOX10	Sensitive	3.42	0	4.56	0	11.21	0
LEF1	Sensitive	4.19	0	5.79	0	7.60	0
A. Computational results							

	Role	logFC	t-value	p-value	adj.p-value
EGFR	Resistant	3.87	29.54	2.55E-06	5.04E-04
PDGFRB	Resistant	2.50	15.39	4.64E-05	2.11E-03
MET	Resistant	3.42	20.83	1.21E-05	1.01E-03
YAP1	Resistant	-0.01	-0.08	9.39E-01	9.64E-01
SOX10	Sensitive	-2.41	-25.44	4.97E-06	6.56E-04
LEF1	Sensitive	-3.37	-37.17	9.11E-07	3.56E-04
B. M229-R5 differential expression.					

	Role	logFC	t-value	p-value	adj.p-value
EGFR	Resistant	3.35	21.83	2.06E-06	5.69E-04
PDGFRB	Resistant	2.35	13.67	2.40E-05	2.18E-03
MET	Resistant	3.36	14.85	1.56E-05	1.71E-03
YAP1	Resistant	0.19	1.20	2.81E-01	5.84E-01
SOX10	Sensitive	-2.53	-16.86	8.03E-06	1.17E-03
LEF1	Sensitive	-2.59	-14.68	1.65E-05	1.77E-03
C. M238-R1 differential expression.					

Table S4. Method comparison based on known genes associated with *BRAF* inhibitor efficacy, Related to Figure 4.

Two previous studies have identified regulator genes of anti-*BRAF* resistance (Hugo et al., 2015; Sun et al., 2014). The type of association with drug efficacy is shown in the first column of each sub-table. If the activation of a gene is associated with a gain of drug resistance, the gene will be classified as "Resistant" markers. In contrast, if the loss of a gene is associated with a gain of drug resistance, the gene will be classified as "Sensitive" markers.

(A) Computational results from CARE and Elastic Net are shown across three cohorts. For CARE t-value, a negative score indicates the gene feature as a resistant marker, and a positive score indicates the gene feature as a sensitive marker.

(B) Differential gene expression between the M229-R5 drug resistant cell line and parental line M229. For these regulator genes, their gene expression values are compared between drug resistant cell lines and sensitive parental lines using the data from a previous study (Nazarian et al., 2010). The differential expression analyses were done with Limma (Ritchie et al., 2015). logFC represents the log-fold change of mRNA level between the drug resistant cell line and its parental sensitive cell line. The t-value was computed as logFC divided by standard deviation

estimated in the linear model. The p-value represents the statistical significance for each t-value, followed with the adjusted p-value after multiple test correction.

(C) Differential gene expression between the M238-R1 drug resistant cell line and parental line M238 as panel B.

A. CARE filtered

ID	CARE			Expression		PCR
	CCLE	**CTRP**	**GDSC**	**BT474**	**SKR6**	
AKT3	-4.41	-3.81	-2.39	6.47	5.15	-0.40
PRKD3	-3.07	-3.39	-3.59	6.60	9.04	-0.82

B. Others

SERPINE1	-5.18	-6.84	1.04	3.95	26.61	-1.74
ADA	-4.67	-2.00	-2.21	4.26	4.36	-1.56
PIM1	-4.02	0.38	-1.90	2.12	5.94	-0.36
SOAT1	-2.59	-3.19	0.33	2.17	8.30	-0.44
MAOA	-1.93	0.71	1.80	6.32	3.10	-0.35
JAK2	-1.16	0.29	-2.29	2.28	4.80	-1.20
PTGES	-0.61	-1.71	-0.34	39.00	12.87	-2.10
ABCG2	-0.37	-1.93	-5.31	3.42	29.17	-0.46
CYP1A2	-0.31	3.02	-2.55	3.86	14.56	-0.36
SLC6A4	0.21	1.96	-3.06	2.46	10.47	-1.35
BTK	1.33	-0.03	-1.86	3.29	3.78	-1.06
PAK6	2.62	2.69	1.89	3.07	9.25	-1.02

Table S5. Druggable genes associated with lapatinib resistance, Related to Figure 5.

The first group of CARE score was computed using data from three compound screen cohorts. The second group ("Expression") of t-values are from Limma results, testing the differential gene expression between Lapatinib resistant cell line and parental line. The third group of t-values was calculated using Limma, testing the association between gene level and patient pathological complete response (pCR) status. All genes shown have commercial inhibitors available.

(A) Genes with consistently significant CARE scores.

(B) Other genes without the requirement of consistently significant CARE scores, with genes shown in panel A excluded.

References

Hugo, W., Shi, H., Sun, L., Piva, M., Song, C., Kong, X., Moriceau, G., Hong, A., Dahlman, K.B., Johnson, D.B.*, et al.* (2015). Non-genomic and Immune Evolution of Melanoma Acquiring MAPKi Resistance. Cell *162*, 1271-1285.

Konermann, S., Brigham, M.D., Trevino, A.E., Joung, J., Abudayyeh, O.O., Barcena, C., Hsu, P.D., Habib, N., Gootenberg, J.S., Nishimasu, H.*, et al.* (2015). Genome-scale transcriptional activation by an engineered CRISPR-Cas9 complex. Nature *517*, 583-588.

Manguso, R.T., Pope, H.W., Zimmer, M.D., Brown, F.D., Yates, K.B., Miller, B.C., Collins, N.B., Bi, K., LaFleur, M.W., Juneja, V.R.*, et al.* (2017). In vivo CRISPR screening identifies Ptpn2 as a cancer immunotherapy target. Nature.

Nazarian, R., Shi, H., Wang, Q., Kong, X., Koya, R.C., Lee, H., Chen, Z., Lee, M.K., Attar, N., Sazegar, H.*, et al.* (2010). Melanomas acquire resistance to B-RAF(V600E) inhibition by RTK or N-RAS upregulation. Nature *468*, 973-977.

Ritchie, M.E., Phipson, B., Wu, D., Hu, Y., Law, C.W., Shi, W., and Smyth, G.K. (2015). limma powers differential expression analyses for RNA-sequencing and microarray studies. Nucleic acids research *43*, e47.

Subramanian, A., Tamayo, P., Mootha, V.K., Mukherjee, S., Ebert, B.L., Gillette, M.A., Paulovich, A., Pomeroy, S.L., Golub, T.R., Lander, E.S.*, et al.* (2005). Gene set enrichment analysis: a knowledge-based approach for interpreting genome-wide expression profiles. Proceedings of the National Academy of Sciences of the United States of America *102*, 15545-15550.

Sun, C., Wang, L., Huang, S., Heynen, G.J., Prahallad, A., Robert, C., Haanen, J., Blank, C., Wesseling, J., Willems, S.M.*, et al.* (2014). Reversible and adaptive resistance to BRAF(V600E) inhibition in melanoma. Nature *508*, 118-122.